THE JOURNAL OF BIOLOGICAL CHEMISTRY VOL. 285, NO. 42, pp. 32504–32511, October 15, 2010

Structure and Metal Loading of a Soluble Periplasm Cuproprotein*[S]

Received for publication, June 9, 2010, and in revised form, July 21, 2010 Published, JBC Papers in Press, August 10, 2010, DOI 10.1074/jbc.M110.153080

Kevin J. Waldron[1], Susan J. Firbank[1], Samantha J. Dainty, Mónica Pérez-Rama, Steve Tottey[1], and Nigel J. Robinson[2]

From the Institute for Cell and Molecular Biosciences, University of Newcastle Medical School, Newcastle upon Tyne NE2 4HH, United Kingdom

A copper-trafficking pathway was found to enable Cu^{2+} occupancy of a soluble periplasm protein, CucA, even when competing Zn^{2+} is abundant in the periplasm. Here, we solved the structure of CucA (a new cupin) and found that binding of Cu^{2+}, but not Zn^{2+}, quenches the fluorescence of Trp^{165}, which is adjacent to the metal site. Using this fluorescence probe, we established that CucA becomes partly occupied by Zn^{2+} following exposure to equimolar Zn^{2+} and Cu^{2+}. Cu^{2+}-CucA is more thermodynamically stable than Zn^{2+}-CucA but $k_{(Zn \rightarrow Cu)exchange}$ is slow, raising questions about how the periplasm contains solely the Cu^{2+} form. We discovered that a copper-trafficking pathway involving two copper transporters (CtaA and PacS) and a metallochaperone (Atx1) is obligatory for Cu^{2+}-CucA to accumulate in the periplasm. There was negligible CucA protein in the periplasm of Δ*ctaA* cells, but the abundance of *cucA* transcripts was unaltered. Crucially, Δ*ctaA* cells overaccumulate low M_r copper complexes in the periplasm, and purified apoCucA can readily acquire Cu^{2+} from Δ*ctaA* periplasm extracts, but *in vivo* apoCucA fails to come into contact with these periplasmic copper pools. Instead, copper traffics via a cytoplasmic pathway that is coupled to CucA translocation to the periplasm.

Metals diffuse through porins in the outer membrane of Gram-negative bacteria such that the periplasm is exposed to metals from the external medium (1, 2). This raises questions about how the correct metals are acquired by proteins such as CucA, which are exported in an unfolded state by the general secretory pathway and obtain metal after membrane translocation. We previously identified the most abundant Cu^{2+} and Mn^{2+} proteins, CucA and MncA, respectively, in the periplasm of the cyanobacterium *Synechocystis* PCC 6803 (3). MncA has Mn^{2+}-dependent oxalate decarboxylase activity, and CucA shows some Cu^{2+}-dependent quercetin dioxygenase activity. Folding of MncA in an extract of the soluble components of the periplasm aberrantly generates Zn^{2+}-MncA, but MncA is a Tat substrate, which folds prior to export (4–7), and so MncA can acquire Mn^{2+} in the cytoplasm but not the periplasm. Electron paramagnetic resonance spectra of Cu^{2+}-MncA and Cu^{2+}-CucA are closely similar, consistent with similarly determined and deduced metal-binding sites, respectively (3). Because CucA is exported by the general secretory pathway, if its metal-binding site is identical to MncA, then CucA might be predicted to erroneously acquire Zn^{2+} upon folding in the periplasm. Here, we confirm the prediction that CucA will readily bind Zn^{2+} and would be liable to aberrantly acquire Zn^{2+} rather than Cu^{2+} from the exchangeable metal pools in the periplasm.

It has been proposed that copper was recruited during evolution after the appearance of atmospheric dioxygen and then exploited in the development of multicellular eukaryotes (8). It is unclear whether or not copper is needed in the cytosol of most bacteria. Moreover, few if any copper importers have been identified in bacteria. *In vivo* evidence that some P-type ATPases import copper (9–14) has not yet been substantiated with biochemical data *in vitro*. In eukaryotes, copper proteins are extracellular or located within cytoplasmic compartments such as the *trans*-Golgi, vesicles derived from this network, mitochondria, or chloroplasts (15–20). Copper-zinc superoxide dismutase is a rare example of a copper protein found within the eukaryotic cytosol, and it has a copper-delivery protein CCS (21, 22). It is hypothesized that trafficking copper to its destinations by ligand exchange via copper metallochaperones (23, 24), coupled with compartmentalization, minimizes deleterious side reactions in the cytosol (3). A zeptomolar copper affinity of the copper sensor CueR implies that copper is either excluded or tightly bound and buffered within the *Escherichia coli* cytoplasm (25). In bacteria, copper-zinc superoxide dismutase is always extracellular or located within the periplasm, whereas other bacterial copper proteins are membranous, periplasmic, or extracellular. One known cytoplasmic bacterial copper enzyme is particulate methane monooxygenase (26); however, particulate methane monooxygenase is housed in unusual internal membranes (27). Bacteria appear to have avoided the challenges associated with handling copper in the cytoplasm by excluding copper proteins. However, here we discover that the periplasmic copper protein CucA does not obtain its metal from periplasmic pools but requires that copper be first trafficked through the cytoplasm.

The first crystal structures of CucA now confirm a monocupin fold and the coordination of Cu^{2+} via a His_3 Glu_1 ligand set,

* This work was supported by Biotechnology and Biological Sciences Research Council PMS Committee Grants BBS/B/02576 and BB/E001688/1.

[S] The on-line version of this article (available at http://www.jbc.org) contains supplemental Tables 1 and 2 and Figs. 1–5.

The atomic coordinates and structure factors (codes 2XL7, 2XL9, 2XLA, 2XLF, and 2XLG) have been deposited in the Protein Data Bank, Research Collaboratory for Structural Bioinformatics, Rutgers University, New Brunswick, NJ (http://www.rcsb.org/).

[1] These authors contributed equally to this work.

[2] To whom correspondence and requests for materials should be addressed. E-mail: n.j.robinson@ncl.ac.uk.

analogous to the Mn^{2+}-binding residues of MncA. Trp^{165} is proximal to the metal-binding site, and its fluorescence is quenched by Cu^{2+} but not by Zn^{2+}, allowing metal binding to be followed spectrally. *In vitro* metallation studies reveal ~50% initial occupancy with Zn^{2+} after exposure of apoCucA to an equimolar mixture of Cu^{2+} and Zn^{2+}, followed by a slow (>24 h to equilibrium) exchange to 100% Cu^{2+}-CucA. CucA was previously identified via the fractionation of periplasm extracts using two-dimensional native liquid chromatography followed by metal analysis using inductively coupled plasma mass spectrometry (ICP-MS)[3] (3). By this approach, it is possible to quantify the number of atoms of copper bound to CucA per cell. Here, the same method has been used to quantify the number of atoms of copper associated with CucA in mutants deficient in genes known to encode proteins of copper homeostasis (9, 12, 28, 29). Accumulation of Cu^{2+}-CucA *in vivo* requires the same three proteins PacS, CtaA, and Atx1, which supply copper to plastocyanin within internal thylakoid compartments. Low M_r Cu^{2+} pools increase in abundance in periplasm extracts of Δ*pacS*, Δ*ctaA*, and Δ*atx1* mutants, in which Cu^{2+}-CucA fails to accumulate, showing that CucA does not directly acquire Cu^{2+} from these periplasmic pools. The abundance of CucA protein, but not transcripts, declines in a copper-trafficking mutant. Thus, the copper pathway does not act on expression of the *cucA* gene but assists the metal supply to CucA itself, and moreover, the copper supply is linked to CucA accumulation in the periplasm.

EXPERIMENTAL PROCEDURES

General Reagents and Bacterial Cultures—*Synechocystis* PCC 6803 was cultured at 28 °C under constant light in standard BG-11 medium. Mutant strains Δ*ctaA* (9), Δ*pacS* (9), and Δ*atx1* (28) were described previously and were maintained in the presence of kanamycin (50 μg ml^{-1}) or chloramphenicol (7.5 μg ml^{-1}), but antibiotics were omitted from the final experimental cultures to prevent metal chelation effects.

E. coli BL21(DE3) cells (Novagen) were cultured in Luria-Bertani (LB) medium, and B834(DE3) cells (Novagen) were cultured in M9 minimal medium containing seleno-L-methionine (Sigma). The pET29a plasmid (Novagen) was maintained by including kanamycin (50 μg ml^{-1}) where necessary.

CucA Production, Purification, and in Vitro Metal Binding Studies—Cloning of the *cucA* gene for heterologous expression was described previously (3). Site-directed mutagenesis of Trp^{165} to Phe was achieved using the QuikChange method (Stratagene) with the primers 5′-CGGATAAAACATTACCCATTGTTTTTGTTTTCATGCGTAATGAAGTTGCACCGG-3′ and 5′-CCGGTGCAACTTCATTACGCATGAAAACAAAAACAATGGGTAATGTTTTATCCG-3′. Resulting colonies were screened for the loss of a BtsCI restriction site, and a successful clone was verified by sequencing. The expression, refolding, and purification of recombinant CucA protein was performed essentially as described previously (3), except that the final size exclusion chromatography step utilized a HiLoad 26/60 Superdex 200 column (GE Healthcare). The anion exchange-concentrated refolded protein, in 50 mM Tris, pH 7.5, 500 mM NaCl, 10 mM EDTA, was resolved on the size exclusion column in 10 mM HEPES, pH 7.0, 150 mM NaCl at 0.5 ml min^{-1} at 4 °C, collecting 5-ml fractions. CucA-containing fractions were assayed for protein by Coomassie assay (Pierce), and CucA was quantified by UV-visible spectroscopy (Cary 4E) using the calculated $\epsilon_{280\,nm}$ = 32,890 M^{-1} cm^{-1} for wild type and 27,930 M^{-1} cm^{-1} for the W195F mutant. Protein was verified to be metal-free (designated as containing <0.05 mol eq total) by ICP-MS.

Fluorescence spectra were collected using a Cary Eclipse spectrofluorimeter at 20 °C. The excitation wavelength was 280 nm throughout with a 5-nm slit width, and emission was monitored between 300 and 450 nm with a 5-nm slit width, a scan rate of 120 nm min^{-1}, 1-nm data interval, and 0.5-s averaging time. All samples contained ~5 μM CucA in 10 mM HEPES, pH 7.0, 150 mM NaCl in quartz cuvettes (Hellma). All samples were thermally equilibrated for 10 min prior to the experiment. For titrations, metals were added by pipette from concentrated aqueous stock solutions of $CuSO_4$, $ZnSO_4$, or $MnCl_2$, mixed vigorously, and then incubated at 20 °C for 60 s before the spectra were collected. All metal stocks were calibrated by ICP-MS before use. For kinetics experiments, metal was added directly to the cuvette within the spectrometer and rapidly mixed by pipetting. Emission at 320 nm was measured at 1 Hz for the duration of the experiment.

Determination of CucA Crystal Structures—Purified recombinant CucA (apo or metallated) was concentrated to ~10 mg ml^{-1} and buffer-exchanged into 10 mM HEPES, pH 7.0, 50 mM NaCl using a YM-10 centrifugal concentrator (Centricon, Amicon). Initial crystallization trials were set up as sitting drops using a Mosquito robot (TTP Labtech) and commercially available precipitant screens. Conditions yielding crystals were scaled up and optimized in standard 24-well plates using the hanging drop method of vapor diffusion. All crystallization experiments were maintained at 20 °C. Diffraction quality crystals were produced from multiple conditions containing 0.1 M either HEPES or Tris, pH 7.5–8.8, 18–24% (w/v) PEG 8000, at a protein to precipitant solution ratio of 2 μl of protein solution to 1 μl of precipitant solution. For metallated protein, 0.5 mM $CuSO_4$ or 0.5 mM $ZnSO_4$ was included in the precipitant solution or 1 mM EDTA for apoprotein. Prior to data collection, crystals were flash-frozen in liquid nitrogen using the precipitant solution supplemented with 25% glycerol as a cryoprotectant. Data collection statistics and beamlines are listed in supplemental Table 1.

Single wavelength anomalous dispersion was used to solve the crystal structure of the zinc-containing form of SeMet-substituted recombinant CucA to 2.2 Å; crystals of Cu^{2+}-SeMet-CucA were obtained but were much smaller and did not diffract as far. Although sufficient anomalous data were collected from the copper form to permit structure solution (data not presented), the zinc structure was used as a molecular replacement model for the other CucA structures, including Cu^{2+}-SeMet-CucA. The structure of Zn^{2+}-CucA-SeMet was solved using the SHELX C/D/E programs as part of CCP4i. The resulting phases were used as starting phases in RESOLVE, which built the majority of the protein. The model building was

[3] The abbreviations used are: ICP-MS, inductively coupled plasma mass spectrometry; ASU, asymmetric unit; SeMet, selenomethionine.

completed manually in COOT with refinement carried out using Refmac5. Molecular replacement was subsequently carried out using MOLREP. Models were validated using the MOLPROBITY webserver. Structures were aligned for comparisons using LSQMAN or THESEUS. The majority of structures were obtained in the closed form; however, particularly the apoprotein or Cu^{2+}-CucA crystallized in the absence of excess metal crystallized readily in the open form. No correlation was observed between crystal forms and the pH of the precipitant solution. The presence of copper or zinc was confirmed by calculation of anomalous difference maps from data collected at 1.378 or 1.282 Å, respectively, and by the collection of energy scans across the copper/zinc region at ESRF beamline ID29-1.

Analysis of Copper Complexes in Periplasmic Extracts—Isolation of periplasmic extracts from *Synechocystis* PCC 6803, two-dimensional liquid chromatography, ICP-MS metal analysis, SDS-PAGE, and MALDI-TOF-MS peptide mass fingerprinting used methods described previously (3), except that HEPES buffer was used throughout in place of Tris buffer used previously.

Isolation of RNA and Reverse Transcriptase-PCR—Total RNA was isolated from logarithmically growing wild-type, Δ*ctaA*, Δ*pacS*, and Δ*atx1* cells using an established method (30). RNA was treated with DNase I (Sigma), and then 1 μg of DNase-treated RNA was used for the production of cDNA using an Im-PromII reverse transcription kit (Promega). Reverse transcriptase was omitted from reaction mixtures that were used as negative controls in the RT-PCR analysis. For the PCR, specific primers for *petE* (forward 5′-TGCCGCTGCCAATGCAACAG-3′ and reverse 5′-GTTCACAGTAGTAGGTGTAG-3′), *petJ* (forward 5′-CTGTGCCGCTTGTCATAATG-3′ and reverse 5′-AGCACGTAGGCCGCCACATC-3′), *cucA* (forward 5′-TATTTTCAAGCTGTGGGGC-3′ and reverse 5′-CGGTTAAAAGCTTCAATTAC-3′), and *rps1* (forward 5′-CTCTGATTGACATTGGGGCG-3′ and reverse 5′-GAGCGCTGATGTGGGAGCCG-3′) were used, which were designed to amplify an ~300-bp region internal to each gene. Cycling conditions, using *Taq* polymerase (New England Biolabs), included an initial denaturation step at 95 °C for 2 min and then 25–30 cycles of denaturation at 95 °C for 1 min, annealing at 60 °C for 1 min and extension at 72 °C for 20 s, followed by a final extension step at 72 °C for 5 min. Products were analyzed on 1% (w/v) agarose gels stained with ethidium bromide.

Metal Association with CucA Using Periplasm Extracts—Periplasm extracts were prepared from 1 to 2 liters of wild-type or Δ*ctaA Synechocystis* PCC 6803 culture, into a final volume of 100 ml of water, as described previously (3). This extract was divided equally into two portions, to which was added 1 ml of 10 mM HEPES, pH 7.0, 150 mM NaCl buffer (denoted "control") or 1 ml of 1.5 μM CucA in the same buffer (denoted "CucA"). The samples were mixed and incubated for 1 h at 4 °C, and then 1 M HEPES, pH 8.8, was added to each sample to a final concentration of 20 mM. Each sample was independently loaded onto a 1-ml HiTrap Q HP anion exchange column (GE Healthcare), washed in 20 ml of 20 mM HEPES, pH 8.8, and then eluted in 1 ml of 20 mM HEPES, pH 8.8, 400 mM NaCl. Aliquots (200 μl) of each eluant fraction were resolved by HPLC size exclusion chromatography (TSK SW3000, Tosoh Biosciences) in 5 mM HEPES, pH 7.0, 50 mM NaCl at 0.5 ml min^{-1} collecting 0.5-ml fractions. Each fraction was analyzed for metal by ICP-MS.

RESULTS

Visualization of the CucA Metal Site Adjacent to Trp_{165}—The structure of CucA was solved, initially for the purpose of visualizing its metal site to identify the metal ligands and to establish whether or not it is a cupin, as predicted through bioinformatics. Diffraction quality crystals of Cu^{2+}-SeMet-CucA (four molecules per asymmetric unit (ASU)), Cu^{2+}-CucA (four and one molecule per ASU), Zn^{2+}-SeMetCucA (two molecules per ASU), and apoSeMetCucA (four molecules per ASU) were analyzed (supplemental Table 1). The Sec-dependent signal sequence of CucA is missing from the recombinant protein, and in addition, four amino-terminal residues were not detected in the electron density maps so that the structures commence at residue 35. CucA is confirmed to exhibit a monocupin fold with the metal-binding site positioned within a relatively hydrophobic cavity (Fig. 1*a*). In metal-bound forms, Cu^{2+} or Zn^{2+}, the metal ion is coordinated to the same four residues, three histidines, $His^{88,90,149}$, plus Glu^{95} (Fig. 1*b*), identical to the protein metal-binding ligands of Mn^{2+}-MncA (3). Bonds to Cu^{2+} and Zn^{2+} are ~2.1 Å (respective metal identities confirmed at edge wavelengths of 1.378 and 1.282 Å) (Fig. 1, *c* and *d*). Trp^{165} is proximal to the metal at 4.4 Å (Fig. 1*b*), and therefore, its fluorescence is liable to be quenched through Förster dipole coupling of the Trp excited state with metal-derived charge transfer transitions of suitable energies (31).

The metal binding geometry of both Cu^{2+}-CucA and Zn^{2+}-CucA to protein ligands approximates to distorted tetrahedral arrangement, but one or two water molecules provide additional fifth and possibly sixth ligands at variable distances. One water molecule is at a comparable distance to the other ligands (1.9–2.4 Å), and the second tends to be longer, perhaps not coordinating at all (2.4–3.2 Å), generating a distorted square pyramidal arrangement. Cu(II) has a preference for square planar or square pyramidal Zn(II) for tetrahedral geometry, and hence CucA imposes a geometry that may influence its metal-binding preferences. The surrounding protein structure is comparable between the two metal forms (Cu^{2+} *versus* Zn^{2+}). More than one crystal conformer of CucA was observed (supplemental Fig. 1), with some analogy to the open and closed forms of oxalate decarboxylase (32, 33). Both open and closed conformations of Cu^{2+}-CucA have been detected. The open forms contain a channel to the metal-binding site that is expected to allow substrate entry and product release. Although the endogenous substrates of Cu^{2+}-CucA are unknown, the enzyme exhibits some quercetin dioxygenase activity that is absent in Zn^{2+}-CucA (3). However, the channel to the CucA metal site and the presumed substrate cavity is small compared with known quercetin dioxygenases (34), suggesting that the *in vivo* substrate is likely to be smaller than quercetin. The entry pocket is lined by Glu^{58}, Phe^{60}, Pro^{85}, and Phe^{209} with a single string of water molecules connecting the metal site to the surface (supplemental Fig. 2). In the alternative

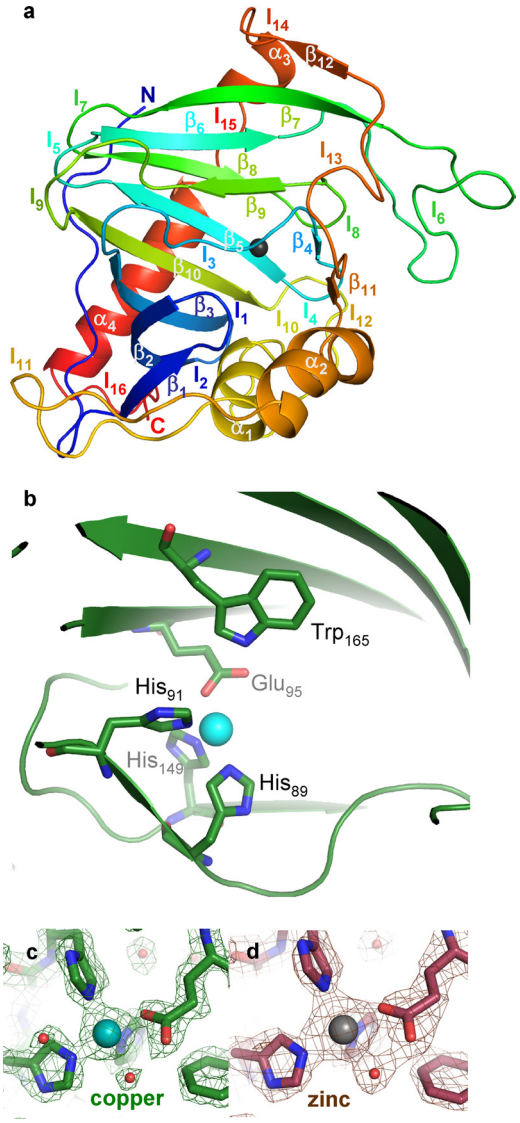

FIGURE 1. **Crystal structure of Cu^{2+}-CucA.** *a,* structural elements (α, α-helices; β, β-strands; *l*, loops), colored in order from the amino (*blue*) to carboxyl (*red*) terminus, are numerically labeled. *b,* residues (*green*) surrounding the copper atom (*blue sphere*) of Cu^{2+}-CucA are shown in the closed conformation. *c,* residues surrounding the metal atoms within CucA with corresponding composite omit electron density maps each contoured at 1.5 σ for Cu^{2+}-CucA, and *d,* Zn^{2+}-CucA.

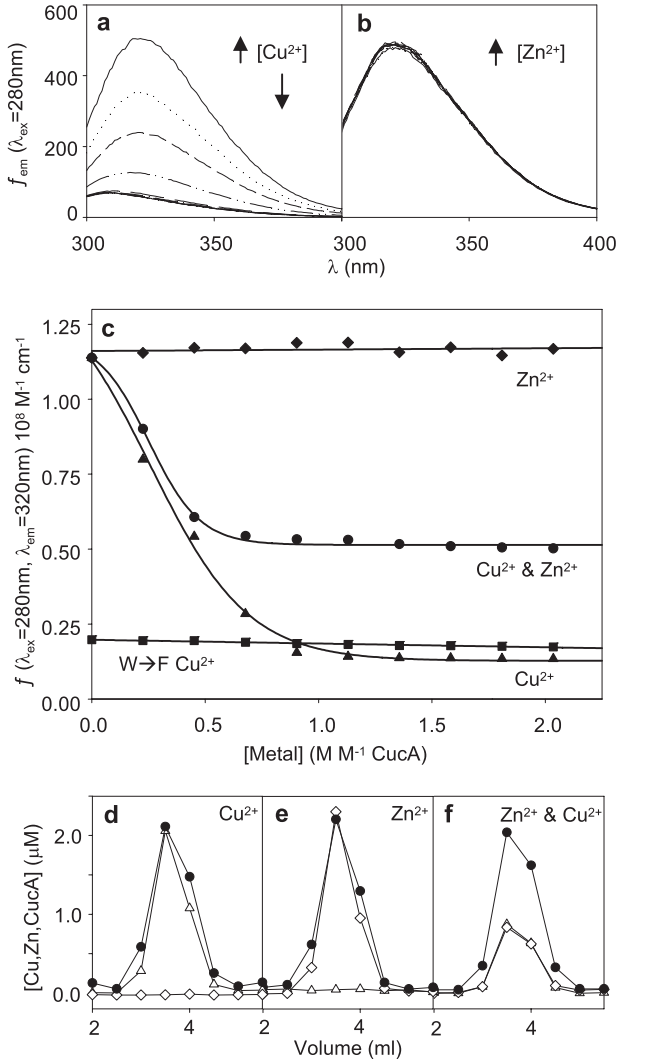

FIGURE 2. **Copper and zinc both bind to CucA.** *a,* quenching of the fluorescence emission spectra of CucA (5 μM in 10 mM HEPES, pH 7.0, 150 mM NaCl) exposed to increasing concentrations of Cu^{2+}, 280 nm excitation. *b,* lack of quenching of the fluorescence emission spectra of CucA, as in *a*, exposed to increasing concentrations of Zn^{2+}. *c,* fluorescence emission of CucA at 320 nm as a function of added Zn^{2+} (*diamonds*), Cu^{2+} (*triangles*), and simultaneous addition of equimolar Zn^{2+} plus Cu^{2+} to 5 μM apoCucA (*circles*). Fluorescence was measured 60 s after metal addition and mixing. Fluorescence emission of a CucA W165F variant was also determined (*closed squares*). Fractionation of CucA-bound metal by size exclusion chromatography with metal (*open diamonds,* zinc; *open triangles,* copper) detected by ICP-MS after addition of 10 μM Cu^{2+} (*d*), 10 μM Zn^{2+} (*e*), and 10 μM Zn^{2+} plus 10 μM Cu^{2+} (*f*) to 5 μM apoCucA (*closed circles*, protein).

form of CucA, the channel is occluded by the movement of residues 52–60, resulting in Glu^{58} and Ala^{56} and the loop 1 region projecting into the channel (supplemental Fig. 3). The *B*-factors are higher in open CucA, notably in the regions that close the channel in the alternative form (supplemental Fig. 4), and several residues (203–207 inclusive) from helix α2 and loop 11 could not be modeled in this open form.

Binding of Cu^{2+} and Zn^{2+} to CucA in Vitro—In vitro metal-binding experiments previously suggested that MncA might prefer Zn^{2+} relative to Cu^{2+}, with approximately 1 order of magnitude difference in stability constants (3). Because the CucA ligands are identical to those of MncA (Fig. 1*b*) its preference for Cu^{2+} relative to Zn^{2+} was therefore tested (Fig. 2). Intrinsic fluorescence of CucA is quenched by 1 eq of Cu^{2+} (Fig. 2*a*) but not Zn^{2+} (Fig. 2*b*), although CucA does bind 1 eq of Zn^{2+} (Fig. 2*e*). Cu^{2+}-dependent quenching was lost when Trp^{165} was substituted with Phe, and this CucA variant had a low level of fluorescence similar to that of wild-type CucA saturated with Cu^{2+} (Fig. 2*c*). These data support Trp_{165} as the source of fluorescence that is quenched by Cu^{2+}. Unlike Zn^{2+}, which is spectrally silent due to its d_{10} electron configuration, charge transfer transitions are common with Cu^{2+}. Quenching of fluorescence by Cu^{2+}, but not Zn^{2+}, is thus consistent with a Förster dipole coupling mechanism.

Metallation of apoCucA with equimolar Zn^{2+} and Cu^{2+} initially causes only partial quenching of fluorescence (Fig. 2*c*). The initial generation of a mixture of Zn^{2+}-CucA and Cu^{2+}-CucA was confirmed by analyzing bound metal by ICP-MS after fractionation by size exclusion chromatography (Fig. 2*f*).

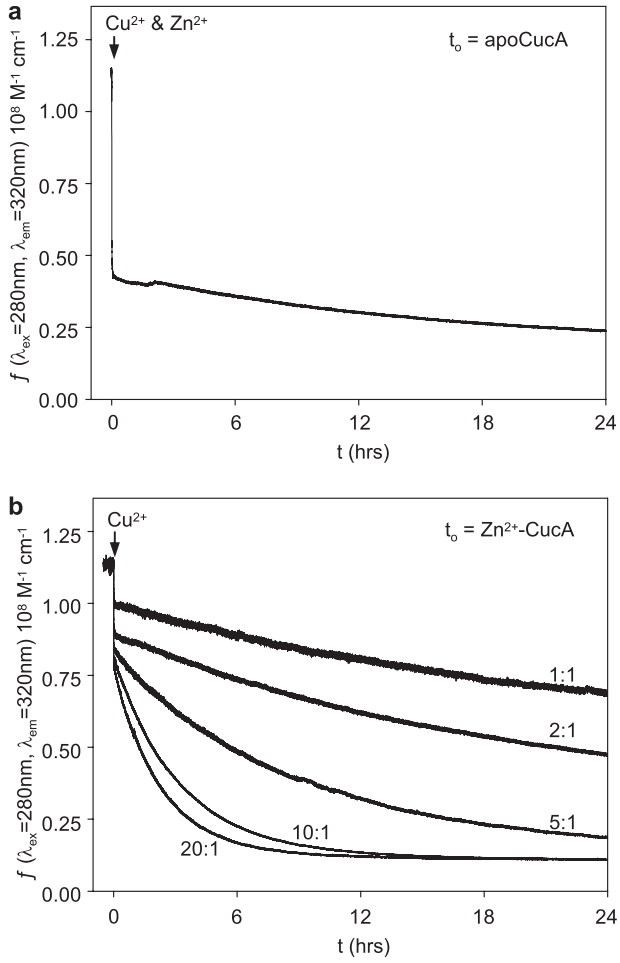

FIGURE 3. **Zn^{2+}-CucA exchanges slowly with Cu^{2+}.** *a,* quenching of the fluorescence emission of apoCucA (5 μM) as a function of time following simultaneous addition of equimolar Zn^{2+} and Cu^{2+} (both at 2.5 M excess with respect to CucA). *b,* quenching of the fluorescence emission of Zn^{2+}-CucA (2.5 M excess relative to CucA) as a function of time following addition of Cu^{2+} at increasing molar eq relative to Zn^{2+} (1:1, 2:1, 5:1, 10:1, and 20:1).

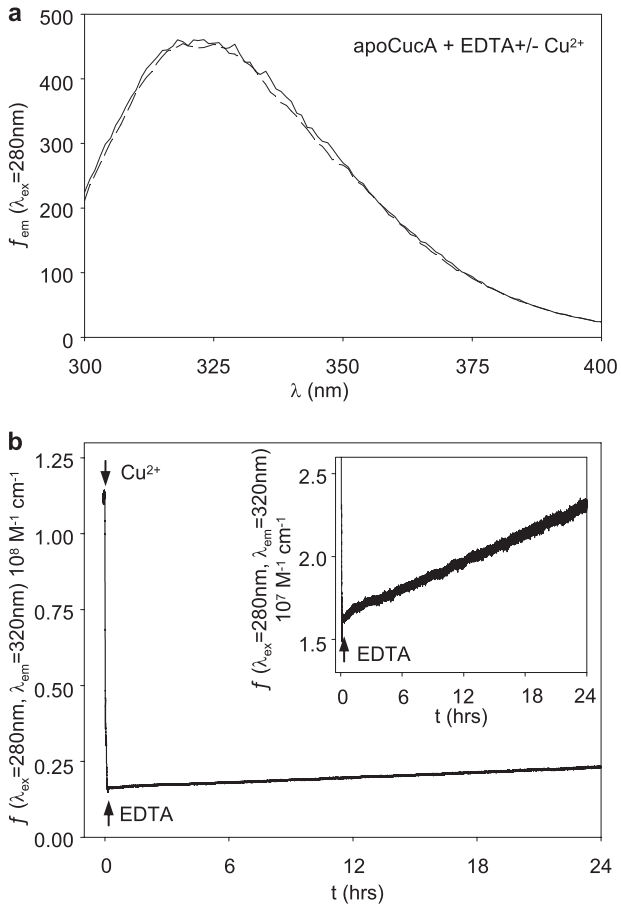

FIGURE 4. **Dissociation of Cu^{2+}-CucA is slow.** *a,* intrinsic fluorescence of CucA (5 μM) is not quenched by 2.5 M excess Cu^{2+} added in the presence of EDTA (1 mM). *b,* slow restoration of intrinsic fluorescence of CucA after initial quenching with 2.5 M eq of Cu^{2+} followed by the addition of excess EDTA (1 mM). *Inset* is plotted on an expanded *y* axis to show the rate of Cu^{2+}-CucA dissociation.

Prolonged incubation for 24 h leads to further quenching approaching that observed following the addition of Cu^{2+} alone (Fig. 3*a*). This implies slow Zn^{2+} to Cu^{2+} exchange, with Cu^{2+} ultimately forming the more thermodynamically stable complex at equilibrium. The rate of replacement of Zn^{2+} by Cu^{2+} is concentration-dependent (Fig. 3*b*). EDTA (1 mM) out-competes apoCucA (5 μM) for Cu^{2+} (Fig. 4*a*), and a dissociation rate for Cu^{2+}-CucA of $k_{Cu,OFF} = 7.5 \times 10^{-7}\ s^{-1}$ was thus estimated from the rate of increase in Cu^{2+}-CucA fluorescence in the presence of a similar excess of EDTA (Fig. 4*b*). The initial formation of an approximately equal mixture of Zn^{2+}-CucA and Cu^{2+}-CucA (Fig. 2*f*) implies that the two metals have similar association rates, and therefore a dissociation rate for Zn^{2+}-CucA of $k_{Zn,OFF} = 4.6 \times 10^{-5}\ s^{-1}$ was estimated from the rate of metal exchange in the presence of surplus Cu^{2+} (Fig. 3*b*). A similar value of $k_{Zn,OFF} = 5.0 \times 10^{-5}\ s^{-1}$ was also estimated by detecting loss of Zn^{2+} from CucA by ICP-MS after 48 h (data not shown).

Thus, the metal site of CucA prefers Cu^{2+} to Zn^{2+}, but if Zn^{2+} binds first, the subsequent replacement with Cu^{2+} is slow. Under these biochemical/biophysical conditions, partial occupancy with Zn^{2+} might be predicted to occur *in vivo* at times when the periplasm does not contain a sufficient excess of Cu^{2+} relative to Zn^{2+}. In natural environments periplasm Cu^{2+} levels are likely to be much more limiting than in nutrient-rich BG-11 culture medium that contains 0.3 μM copper. Conversely, BG-11 medium contains a surplus of zinc relative to copper, yet CucA is occupied by copper.

Copper Transporters CtaA and PacS, Plus the Atx1 Metallochaperone, Are Required for Formation of Cu^{2+}-CucA—Copper is required for plastocyanin and cytochrome oxidase in this bacterium, both of which are located within internal membrane-bound compartments called thylakoids (Fig. 5*a*). Mutants deficient in either of two P_1-type ATPases, CtaA and PacS, or a soluble metallochaperone Atx1 (Fig. 5*a*), show phenotypes consistent with impaired copper supply to these cytoplasmic enzymes (9, 28). Here, we have used native two-dimensional liquid chromatography followed by inductively coupled plasma-mass spectrometry of periplasm extracts to compare the number of atoms of Cu^{2+} bound to CucA per cell, in the Δ*atx1*, Δ*ctaA*, and Δ*pacS* mutants (Fig. 5, *b* and *c*). The Cu^{2+} pool in periplasm extracts corresponding to CucA was identified previously by mass fingerprinting after using principal component analysis to correlate Cu^{2+} with proteins that had been further resolved using denaturing PAGE (3). Here, we find

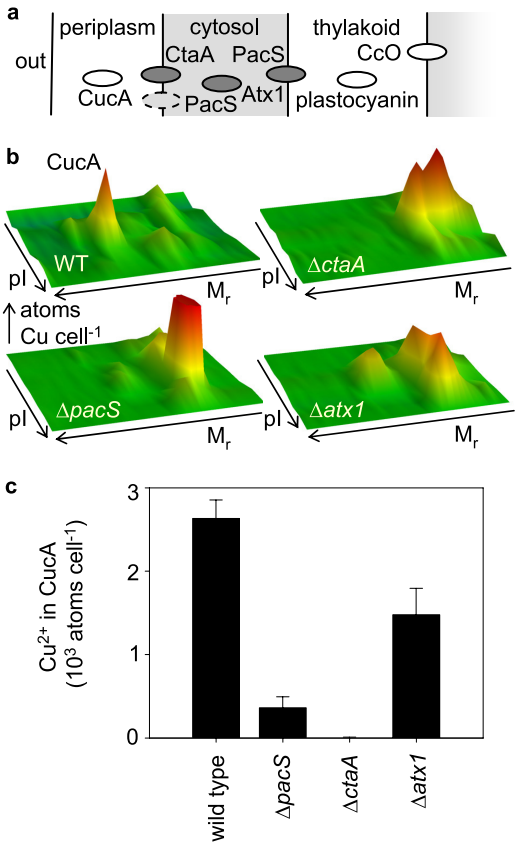

FIGURE 5. **CucA obtains less Cu^{2+} in trafficking mutants.** *a*, cuproproteins CucA, plastocyanin and cytochrome oxidase (CcO), are located in the periplasm and thylakoid compartments, respectively. Copper metallochaperone Atx1 is cytosolic and interacts with amino-terminal regions of copper ATPases CtaA and PacS. PacS is predominantly located in thylakoid membranes. *b*, profile of periplasmic copper complexes from wild-type and mutant cells, separated using two-dimensional liquid chromatography based on relative molecular mass (M_r) and charge (pI). *c*, number of atoms of Cu^{2+} $cell^{-1}$ bound to CucA in wild-type and mutant cells calculated from the volumes under CucA peaks (as in *b*). Data are the means of three independent replicates with S.D. of triplicates.

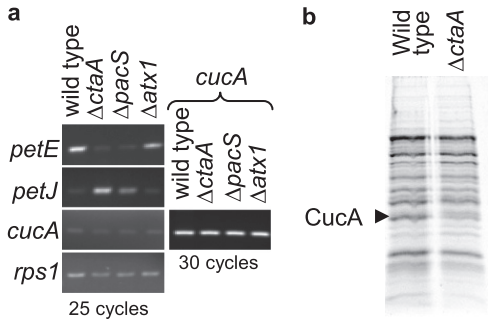

FIGURE 6. **Loss of CucA protein but not transcripts in Cu^{2+}-trafficking mutants.** *a*, RT-PCRs using RNA isolated from the four genotypes and primers corresponding to the four transcripts as shown. All products are reverse transcriptase-dependent (supplemental Fig. 5). 25 cycles, plus 30 cycles for *cucA*, were used. Similar trends were observed in two further experiments using independent RNA isolates. *b*, SDS-PAGE of crude periplasm extracts of wild-type and Δ*ctaA* mutants after concentration using ion exchange chromatography.

that the loss of any of the three proteins that supply copper to plastocyanin also leads to a decline in Cu^{2+}-CucA (Fig. 5, *b* and *c*). The phenotype is weakest for mutants lacking the copper metallochaperone Atx1, implying that its role in the pathway is partly redundant, although in the absence of either of the copper ATPases, CtaA, or PacS, negligible Cu^{2+} reaches CucA. This has some analogy to the loss of cbb_3 oxidase in *Rhodobacter capsulatus* on deletion of the hypothetical copper-ATPase CcoI (13). Notably, the cbb_3 oxidase is a membrane protein with an intramembrane Cu_B site and hence dissimilar to the periplasm localization of CucA.

Expression of the cucA Gene Does Not Respond to Copper—Loss of Cu^{2+}-CucA in Δ*ctaA*, Δ*pacS*, or Δ*atx1* mutant cells could either result from altered expression of the *cucA* gene due to loss of copper supply to a metal-sensing transcriptional regulator or impaired Cu^{2+} delivery to apoCucA. The plastocyanin gene *petE* is switched off in low copper and the cytochrome c_6 gene *petJ* is switched on, to allow the substitution of copper in plastocyanin with heme iron in cytochrome c_6 for photosynthetic electron transport (35, 36). These two genes were therefore used as controls in an analysis of copper-responsive gene expression. No change in the abundance of *cucA* transcripts was detected in any of the mutants, although a decrease in *petE* and an increase in *petJ* transcripts was most evident in cells missing either copper transporter (Fig. 6*a*). This implies that the two transporters and the metallochaperone are involved in Cu^{2+} supply to CucA itself rather than to a transcriptional regulator of the *cucA* gene.

The CucA protein is undetected in a crude periplasm extract from the Δ*ctaA* mutant (Fig. 6*b*). There are at least two similarly migrating bands in the region of CucA on Fig. 6*b*, and mass fingerprinting confirms that these are not CucA in Δ*ctaA* mutants (supplemental Table 2). Loss of CucA protein implies that some facet of the production of CucA, its localization or stability, depends upon acquisition of the correct metal that in turn depends upon a copper-trafficking pathway.

Purified CucA Can Acquire Cu^{2+} from ΔctaA Periplasm Extracts in Vitro—Additional low M_r Cu^{2+}-complexes accumulate in the periplasm of each of the transport and trafficking mutants (Fig. 5*b*). Presumably these represent a source of copper that would normally be imported across the cytoplasmic membrane and trafficked to CucA via the actions of CtaA, Atx1, and PacS. The chemical nature of these low M_r periplasm copper complexes is unknown, but they might include copper-glutathione in the light of evidence of periplasm-localized glutathione (37). We have examined whether or not these complexes could provide a source of copper for CucA by adding purified apoCucA to periplasm extracts and determining the metal status of the recombinant protein. By using extracts from wild-type cells, CucA does acquire some zinc (0.22 mol eq assuming full recovery of CucA) (Fig. 7), supporting the concept that some mechanism will indeed be required to achieve full copper occupancy *in vivo*, especially after growth in natural environments with less copper availability. Most importantly, using similar extracts from Δ*ctaA* mutants, recombinant CucA became fully populated with copper (0.95 eq assuming full recovery of CucA) (Fig. 7), suggesting that the low M_r copper complexes that accumulate in these cells are suitable copper donors yet fail to form Cu^{2+}-CucA in Δ*ctaA* mutants (Fig. 5). Thus, in living cells apoCucA does not directly acquire Cu^{2+} from the low M_r pools in the periplasm, rather these ions must be trafficked through the cytoplasm for Cu^{2+}-

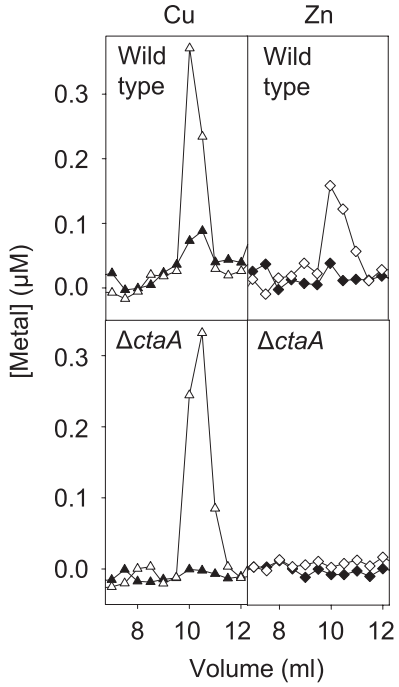

FIGURE 7. ***In vitro* apoCucA acquires copper from Δ*ctaA* but zinc and copper from wild-type periplasm extracts.** Purified CucA protein (1 ml of 1.5 μM in 10 mM HEPES, pH 7.0, 150 mM NaCl) (*open symbols*) or buffer control (*closed symbols*) was added to periplasm extracts, which were then concentrated by anion exchange and eluted metal complexes resolved by gel filtration HPLC (TSK SW-3000) and eluant analyzed for copper (*triangles*) and zinc (*diamonds*) by ICP-MS.

CucA to accumulate in the periplasm implying that transmembrane copper transport is coupled to protein production and/or delivery to the periplasm.

DISCUSSION

Ab initio structures of CucA reveal a monocupin that binds divalent metals via three histidine imidazoles and a glutamate carboxylate within a hydrophobic pocket (Fig. 1). Dissociation rates for Zn^{2+} and Cu^{2+} are slow, in the region of $k_{Zn,OFF} = 4.6 \times 10^{-5}\ s^{-1}$ and $k_{Cu,OFF} = 7.5 \times 10^{-7}\ s^{-1}$, respectively, allowing only slow replacement of Zn^{2+} with Cu^{2+} (Figs. 2–4). Association rates for Zn^{2+} and Cu^{2+} are both rapid ($k_{Zn,ON} \approx k_{Cu,ON}$) such that incubation of apoCucA with equimolar Zn^{2+} and Cu^{2+} generates a mixed population of Zn^{2+}-CucA and Cu^{2+}-CucA that only gradually (t = days) resolves to the more thermodynamically stable Cu^{2+} form (Figs. 2 and 3). Cu^{2+} acquisition *in vivo* is facilitated by a copper-trafficking pathway involving two P_1-type ATPases and copper metallochaperone (Fig. 5), the same proteins also supply copper to plastocyanin within thylakoids (9, 28).

Why is CucA Cu^{2+} acquisition assisted by a trafficking pathway *in vivo*? Maintaining a pool of exchangeable Cu^{2+} in the periplasm, sufficient to correctly populate CucA, would be challenging in natural environments with low concentrations of Cu^{2+}. Presumably, the trafficking pathway encourages occupancy of CucA with Cu^{2+} and not some other metal such as Zn^{2+}. Notably, partial occupancy of apoCucA with Zn^{2+} occurs when apoCucA acquires metal from periplasm extracts of wild-type cells cultured in standard medium that is copper-rich relative to natural habitats (Fig. 7).

CucA is missing from the periplasm of copper-trafficking mutants revealing that cofactor insertion into CucA is necessary for the protein to accumulate (Fig. 6*b* and supplemental Table 2). This is not a function of Cu^{2+}-dependent expression of the *cucA* gene because *cucA* transcripts show normal levels of abundance in both Δ*ctaA* and Δ*pacS* cells (Fig. 6*a*). It is well established that many apoproteins are more susceptible to proteolytic degradation *in vivo* than their metal-bound holo-forms. A reasonable hypothesis might have been that in Δ*ctaA*, Δ*pacS*, and Δ*atx1* mutants, CucA fails to acquire sufficient Cu^{2+} and hence is rapidly degraded in the periplasm. However, mutants in either of the copper-transporting ATPases accumulate additional low M_r copper complexes in the periplasm (Fig. 5*b*). Exchangeable copper pools in extracts of the periplasm can readily donate Cu^{2+} to apoCucA *in vitro*, and this is especially true of the pools in Δ*ctaA* cells (Fig. 7). Periplasm extracts of Δ*ctaA* cells grown in standard (copper-replete) culture medium provide sufficient Cu^{2+} to saturate an aliquot of apoCucA, unlike the partial Zn^{2+} occupancy generated using analogous extracts from wild-type cells (Fig. 7). This strongly argues that apoCucA fails to reach the periplasm in copper-trafficking mutants because any apoCucA that had been translated and translocated in Δ*ctaA* cells should have readily acquired copper and become refractory to proteolysis, yet the protein was not detected.

Cyanobacteria are unlike most bacteria in possessing the internal membrane compartments, thylakoids, that house the copper proteins plastocyanin and cytochrome oxidase (Fig. 5*a*). There is some evidence that vesicle trafficking occurs between the plasma and thylakoid membranes (38, 39), which might suggest that CucA could acquire copper in thylakoids before being trafficked to the periplasm. However, multiple proteomics studies have established that the product of open reading frame *sll1785* (namely CucA) is uniquely localized to the periplasm, never the thylakoids; and furthermore, the Sec-dependent signal sequence of CucA has been exploited in multivariate analyses to distinguish periplasm targeting signals from those of proteins targeted to thylakoids (40). Thus, the implication is that translation and translocation of CucA across the plasma membrane is somehow linked to outward copper transport. Future studies should address the nature of this linkage and why it requires both CtaA and PacS. In the related cyanobacterium *Synechococcus* PCC 7942, PacS was mainly localized to thylakoid membranes by Western blotting using an anti-PacS antiserum, with a smaller subpopulation potentially located at the plasma membranes (29).

Accumulation of low M_r Cu^{2+} pools in the periplasm of mutants missing components of the trafficking pathway (Fig. 5*b*) implies that these pools are the source of copper for the pathway, but crucially copper from these pools is routed in and out of the cytoplasm to form Cu^{2+}-CucA *in vivo*. Prokaryotes, including *E. coli*, that are devoid of known cytosolic cuproproteins and devoid of homologues of known cytosolic copper chaperones (such as CopZ or Atx1) must nonetheless have alternative mechanisms to inhibit deleterious side reactions of copper in the cytosol if these ions must pass through this compartment to supply cuproproteins in the periplasm.

Acknowledgment—We thank Andrew McCarthy, ESRF, Grenoble, France, for collecting scans and data at the edges for metal validation.

REFERENCES

1. Nies, D. H. (2007) in *Molecular Microbiology of Heavy Metals* (Nies, D. H., and Silver, S., eds) pp. 117–142, Springer-Verlag, Heidelberg, Germany
2. Nikaido, H., and Vaara, M. (1985) *Microbiol. Rev.* **49,** 1–32
3. Tottey, S., Waldron, K. J., Firbank, S. J., Reale, B., Bessant, C., Sato, K., Cheek, T. R., Gray, J., Banfield, M. J., Dennison, C., and Robinson, N. J. (2008) *Nature* **455,** 1138–1142
4. Santini, C. L., Ize, B., Chanal, A., Müller, M., Giordano, G., and Wu, L. F. (1998) *EMBO J.* **17,** 101–112
5. Palmer, T., and Berks, B. C. (2003) *Microbiology* **149,** 547–556
6. Keegstra, K., and Cline, K. (1999) *Plant Cell* **11,** 557–570
7. Robinson, C., and Bolhuis, A. (2004) *Biochim. Biophys. Acta* **1694,** 135–147
8. Fraústo da Silva, J. J., and Williams, R. J. (2001) *The Biological Chemistry of the Elements*, Oxford University Press, Oxford, UK
9. Tottey, S., Rich, P. R., Rondet, S. A., and Robinson, N. J. (2001) *J. Biol. Chem.* **276,** 19999–20004
10. Odermatt, A., Krapf, R., and Solioz, M. (1994) *Biochem. Biophys. Res. Commun.* **202,** 44–48
11. Lewinson, O., Lee, A. T., and Rees, D. C. (2009) *Proc. Natl. Acad. Sci. U.S.A.* **106,** 4677–4682
12. Phung, L. T., Ajlani, G., and Haselkorn, R. (1994) *Proc. Natl. Acad. Sci. U.S.A.* **91,** 9651–9654
13. Koch, H. G., Winterstein, C., Saribas, A. S., Alben, J. O., and Daldal, F. (2000) *J. Mol. Biol.* **297,** 49–65
14. Hassani, B. K., Astier, C., Nitschke, W., and Ouchane, S. (2010) *J. Biol. Chem.* **285,** 19330–19337
15. Kaplan, J. H., and Lutsenko, S. (2009) *J. Biol. Chem.* **284,** 25461–25465
16. O'Halloran, T. V., and Culotta, V. C. (2000) *J. Biol. Chem.* **275,** 25057–25060
17. Petris, M. J., Mercer, J. F., Culvenor, J. G., Lockhart, P., Gleeson, P. A., and Camakaris, J. (1996) *EMBO J.* **15,** 6084–6095
18. Lin, S. J., Pufahl, R. A., Dancis, A., O'Halloran, T. V., and Culotta, V. C. (1997) *J. Biol. Chem.* **272,** 9215–9520
19. Robinson, N. J., and Winge, D. R. (2010) *Annu. Rev. Biochem.* **79,** 537–562
20. Setty, S. R., Tenza, D., Sviderskaya, E. V., Bennett, D. C., Raposo, G., and Marks, M. S. (2008) *Nature* **454,** 1142–1146
21. Culotta, V. C., Klomp, L. W., Strain, J., Casareno, R. L., Krems, B., and Gitlin, J. D. (1997) *J. Biol. Chem.* **272,** 23469–23472
22. Changela, A., Chen, K., Xue, Y., Holschen, J., Outten, C. E., O'Halloran, T. V., and Mondragón, A. (2003) *Science* **301,** 1383–1387
23. Banci, L., Bertini, I., Ciofi-Baffoni, S., Kozyreva, T., Zovo, K., and Palumaa, P. (2010) *Nature* **465,** 645–648
24. Furukawa, Y., Torres, A. S., and O'Halloran, T. V. (2004) *EMBO J.* **23,** 2872–2881
25. Rae, T. D., Schmidt, P. J., Pufahl, R. A., Culotta, V. C., and O'Halloran, T. V. (1999) *Science* **284,** 805–808
26. Balasubramanian, R., Smith, S. M., Rawat, S., Yatsunyk, L. A., Stemmler, T. L., and Rosenzweig, A. C. (2010) *Nature* **465,** 115–119
27. Brantner, C. A., Buchholz, L. A., Remsen, C. C., and Collins, M. L. (2000) *Curr. Microbiol.* **40,** 132–134
28. Tottey, S., Rondet, S. A., Borrelly, G. P., Robinson, P. J., Rich, P. R., and Robinson, N. J. (2002) *J. Biol. Chem.* **277,** 5490–5497
29. Kanamaru, K., Kashiwagi, S., and Mizuno, T. (1994) *Mol. Microbiol.* **13,** 369–377
30. Huckle, J. W., Morby, A. P., Turner, J. S., and Robinson, N. J. (1993) *Mol. Microbiol.* **7,** 177–187
31. Whittaker, M. M., Mizuno, K., Bächinger, H. P., and Whittaker, J. W. (2006) *Biophys. J.* **90,** 598–607
32. Anand, R., Dorrestein, P. C., Kinsland, C., Begley, T. P., and Ealick, S. E. (2002) *Biochemistry* **41,** 7659–7669
33. Just, V. J., Stevenson, C. E., Bowater, L., Tanner, A., Lawson, D. M., and Bornemann, S. (2004) *J. Biol. Chem.* **279,** 19867–19874
34. Steiner, R. A., Kalk, K. H., and Dijkstra, B. W. (2002) *Proc. Natl. Acad. Sci. U.S.A.* **99,** 16625–16630
35. Zhang, L., McSpadden, B., Pakrasi, H. B., and Whitmarsh, J. (1992) *J. Biol. Chem.* **267,** 19054–19059
36. Merchant, S., and Bogorad, L. (1986) *Mol. Cell. Biol.* **6,** 462–469
37. Pittman, M. S., Robinson, H. C., and Poole, R. K. (2005) *J. Biol. Chem.* **280,** 32254–32261
38. Schneider, D., Fuhrmann, E., Scholz, I., Hess, W. R., and Graumann, P. L. (2007) *BMC Cell Biol.* **8,** 39–48
39. Nevo, R., Charuvi, D., Shimoni, E., Schwarz, R., Kaplan, A., Ohad, I., and Reich, Z. (2007) *EMBO J.* **26,** 1467–1473
40. Rajalahti, T., Huang, F., Klement, M. R., Pisareva, T., Edman, M., Sjöström, M., Wieslander, A., and Norling, B. (2007) *J. Proteome Res.* **6,** 2420–2434